Inorganic Chemistry

Article

pubs.acs.org/IC

Influence of a Bridging Group and the Substitution Effect of Bis(1,2,4-triazine) N-Donor Extractants on Their Interactions with a Np^{V} Cation

Xia Yang,[†] Yanni Liang,[†,‡] Songdong Ding,[‡] Shoujian Li,[‡] Zhifang Chai,[†,§] and Dongqi Wang*[,†]

[†]CAS Key Laboratory of Nuclear Radiation and Nuclear Energy Techniques, and Multidisciplinary Initiative Center, Institute of High Energy Physics, Chinese Academy of Sciences, Beijing 100049, China

[‡]College of Chemistry, Sichuan University, Chengdu, China

[§]School of Radiation Medicine and Interdisciplinary Sciences (RAD-X), Soochow University, Suzhou 215123, China

Supporting Information

ABSTRACT: The present theoretical study provides a realistic evaluation of the equilibrium structure, reaction modes, and bonding characteristics of a variety of neptunyl complexes formed with bis(triazinyl) N-donor extractants, which differ in their bridging groups such as pyridine, bipyridines, and orthophenanthroline, corresponding to the ligands (L) of tridentate bis(triazinyl)pyridines and tetradentate bis(triazinyl)-bipyridines and bis(triazinyl)-1,10-phenanthrolines (BTPhens), respectively. Our calculations show that coordination of $[NpO_2]^+$ to tetradentate ligands is more favorable than that to tridentate ones no matter in a gas, aqueous, or organic phase. The presence of nitrate ions can enhance the coordination ability of neptunyl and stabilize the neutral $NpO_2L(NO_3)$ complexes in thermodynamics. Our studies indicate that the complexation reaction mode $[NpO_2(H_2O)_n]^+ + L + NO_3^- \rightarrow NpO_2L(NO_3) + nH_2O$ is the most probable at the interface between water and the organic phase. The contribution of an orthophenanthroline bridging group is relatively more pronounced compared to its pyridine counterpart in ligand-exchange reaction. Complexation reactions of hydrated neptunyl with C2-BTPhen and BTPhen assisted by a nitrate ion are favorable thermodynamically, resulting from the least deformation of the ligand and strong complexation stability. The quantum theory of atoms-in-molecules and charge decomposition analysis suggest that electron delocalization and charge transfer are the main reasons responsible for stabilization of the tetradentate complexes and reveal a strong ionic feature of the Np−ligand bonds. Inspection of the frontier molecular orbitals reveals a distinct 5f orbital (Np) interaction with ligand atoms, implying the extent of f-based covalency. Our study may facilitate the rational design of ligands toward the improvement of their binding ability with Np^{V} and more efficient separation of Np in spent nuclear fuels.

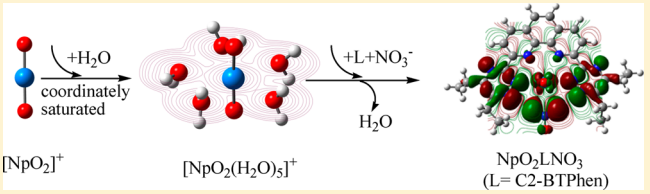

1. INTRODUCTION

There is a great need in developing technologies to separate minor actinides (neptunium, americium, and curium) from post-PUREX (plutonium and uranium extraction) nuclear wastes because of their high radiotoxicity and potential use for other purposes. The practical route is to employ liquid extraction techniques using ligands designed to selectively complex minor actinides. Among nuclear waste products, neptunium (Np) is considered to be one of the most problematic actinide elements in geological disposal,[1] mainly because of one of its isotopes, ^{237}Np, which is an α-emitter with a long half-lifetime [$t_{1/2}(^{237}Np) = 2.14 \times 10^6$ years] with high solubility in groundwater[2] and relatively weak sorption on geological minerals at its most stable oxidation state, Np^{V}.[3,4] Np^{V} predominantly exists as neptunyl cation[3] NpO_2^+. This also makes neptunyl potentially of great environmental and health consequence because it could be readily introduced into the food chain after a waste spill.[5,6] To understand and predict the migration behavior of neptunium in the geological media, neptunyl complexes with the presence of carbonate and sulfate have been the topic of several experimental and theoretical works during the past decade.[7−17] These studies provide a wealth of information to assess the physical and chemical properties of Np; however, up to now, the separation of Np in nuclear waste reprocessing remains a subject to be addressed.

Because O-based ligands show little selectivity for actinides (An) over lanthanides (Ln), a novel family of ligands containing heterocyclic N donors have been developed as potential extractants for minor actinide,[18−25] but most do not survive in low-pH environments, except that one family of bis(triazinyl) ligands can tolerate high acidity.[26,27] Bis(1,2,4-triazine) ligands are unique among N-donor ligands in being able to separate An from Ln under realistic processing conditions with very high selectivities.[27−33] Especially, three classes of ligands have emerged as the most promising for the extraction of minor actinide: the tridentate bis(triazinyl)pyridines (BTPs)[31−33] and the tetradentate bis(triazinyl)bipyridines (BTBPs)[28−30] and bis(triazinyl)-1,10-phenanthrolines (BTPhens),[27,34] as well as their derivatives with several different side chains or substituents attached to the "core" molecule[33,35] for different purposes, for instance, to increase the solubility in the organic phase, to decrease the

Received: January 21, 2014
Published: July 11, 2014

   dx.doi.org/10.1021/ic500138w | Inorg. Chem. 2014, 53, 7848−7860

solubility in the aqueous phase, or to yield a better resistance against radiolysis and hydrolysis. High separation factors of more than 100 for americium (Am) or curium (Cm) versus europium (Eu) were obtained using tridentate BTP ligands in nitric acid systems.[28,32,36−38] The development of the tetradentate BTBP family of extractants is looked at as a breakthrough toward the selective separation of An^{III} [26] and suitable for extracting pentavalent and trivalent elements from tetravalent and hexavalent elements.[39] In addition, the annulated BTBP ($CyMe_4$-BTBP) combines favorable extraction and back-extraction properties of the BTBPs with the enhanced chemical stability of $CyMe_4$-BTP.[26] The tetradentate BTPhen, a new analogue of BTP and BTBP in which the 2,2′-bipyridine moiety of BTBP was replaced by a 1,10-phenanthroline moiety, was reported to separate Am^{III} and Cm^{III} from the lanthanides with remarkably high efficiency, high selectivity, and fast extraction kinetics compared to its 2,2′-bipyridine counterpart.[27,34] Although bis(triazine) ligands are promising toward the separation of trivalent actinides from lanthanides, its performance to extract neptunyl(V) is unclear. Because the separation of neptunyl is important in the development of an advanced nuclear fuel cycle, it is necessary to evaluate potential extractants to be used for neptunyl.

Some studies[18,22,29,33,39−41] suggest the 5f covalency as one of the key factors responsible for the selectivity of An separation with such ligands, while little is known about the exact nature of the covalency in these systems. Therefore, understanding the bonding nature, orbital interaction, charge distribution, and covalency of the interaction between An and various ligands is also important for the rational design of effective ligands for nuclear waste management and spent nuclear fuel reprocessing. To date, it remains a challenge to understand their origin. Recently, it was noted that the ionic/covalent nature of the An−ligand interaction could not be readily identified in population analysis, while the quantum theory of atoms-in-molecules (QTAIM) approach of Bader and co-workers,[42,43] based on topological analysis of the electron density, offers an alternative to complement the characterization of chemical bonding. This method has been used by Kaltsoyannis et al.[40,44−47] to show that there is very little metal−ligand covalency in An complexes. Moreover, it should be pointed out that the strength of bonded interactions should be estimated from the electron density at the bond critical point (BCP) rather than the bond length.[48]

In addition to the metal−ligand covalency, many factors, e.g., the solubility, complexation kinetics, thermodynamic stability, and solvent effects, can contribute to the efficacy of minor An separation. A series of theoretical investigations[23,49−55] have been performed to explore the complexation mechanisms between ligands and heavy-metal ions, and one hypothesis from the experimental[22,28] and theoretical[56,57] studies of BTBPs suggests that it is possible for the ligand-exchange reactions $M(NO_3)_3(H_2O)_4 + L \rightarrow ML(NO_3)_3 + 4H_2O$ (L = BTBPs) and $[M(H_2O)_n]^{3+} + L + 3NO_3^- \rightarrow ML(NO_3)_3 + nH_2O$ to happen at the interface between water and the organic phase. For the bis(triazine) ligands, in the case of neptunyl, only the extraction of Np^V by BTBPs was studied experimentally,[39] in which the reaction process from the aqueous to organic phase remains to be addressed. This makes computational investigations special in the sense to understand the behavior of neptunyl complexes, such as their equilibrium structures, possible complexation modes, bonding characteristics, and the corresponding thermodynamics and kinetics, and to constitute the motivation of the present work, in which the interaction between the chosen model ligands and neptunyl was investigated, including the effect of the bridging group and substituents, with the hope of contributing to the rational design of bis(trizaine) ligands toward the improvement of their binding ability with Np^V.

In the present work, relativistic quantum-chemical calculations were performed to investigate the neptunyl complexes formed by the bis(1,2,4-triazine-3-yl) N-donor family, including the impact of substituents on the geometry, electronic structure, and complexation strength of the involved complexes. The possible modes of the complexation reaction in nitric acid solutions were discussed. In order to reveal the covalency of the metal−ligand dative bond, the qualitative bonding nature of the related neptunyl coordination was characterized by its topological properties using the atoms-in-molecules (AIM) approach,[42,43] the electron localization function (ELF),[58−60] and natural atomic orbital (NAO) analysis.[61] Here, the BTP, BTBP, and BTPhen ligands and their C2 and $CyMe_4$ derivatives were selected as representatives of the bis(1,2,4-triazine-3-yl) N-donor family, as shown in Scheme 1, in which

Scheme 1. General Scheme for Bis(1,2,4-triazine) N-Donor Ligands (L) Studied in This Work[a]

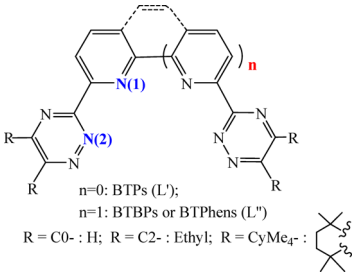

[a]The tridentate and tetradentate ligands are labeled as L′ and L″, respectively.

L′ and L″ refer to the tridentate and tetradentate ligands, respectively. The influence of the solvent effect in aqueous and organic phases was also considered.

2. COMPUTATIONAL DETAILS

All geometry optimization were carried out using the B3LYP,[62−64] Perdew−Burke−Ernzerhof (PBE),[65,66] and Tao−Perdew−Staroverov−Scuseria (TPSS)[67] functionals implemented in the *Gaussian 09* program,[68] representing the hybrid generalized gradient approximation (GGA), GGA, and meta-GGA levels of treatment, respectively. The geometry optimization of An complexes using single-configurational density functional theory (DFT) is generally thought to provide reasonable results.[69−76] The targeted ligands and complex structures were fully optimized without symmetry restrictions. Np was represented by the Stuttgart energy-consistent relativistic effective core potentials, together with a description of the valence shells with a contraction scheme of (14s13p10d8f6g)/[10s9p5d4f3g] (ECP60MWB-SEG basis).[77,78] The split-valence-shell Gaussian basis sets, 6-31G(d),[79] were used to treat the O, N, C, and H atoms for full optimization. The composite basis set is labeled as BS1. The nature of the optimized structures was characterized by vibrational analysis, with which all stationary points were confirmed to be minima and the corresponding zero-point-energy (ZPE) and entropy corrections at room temperature were obtained. All energies reported include ZPE correction. During calculations, because the ligands considered in this work do not bring a ligand field strong enough to enforce a spin flip, the high spin state of a Np^V ion, a triplet, which corresponds to its lowest energy state, was adopted. The $\langle S^2 \rangle$ values were monitored to confirm that there is no spin contamination in the calculations. The

dx.doi.org/10.1021/ic500138w | Inorg. Chem. 2014, 53, 7848−7860

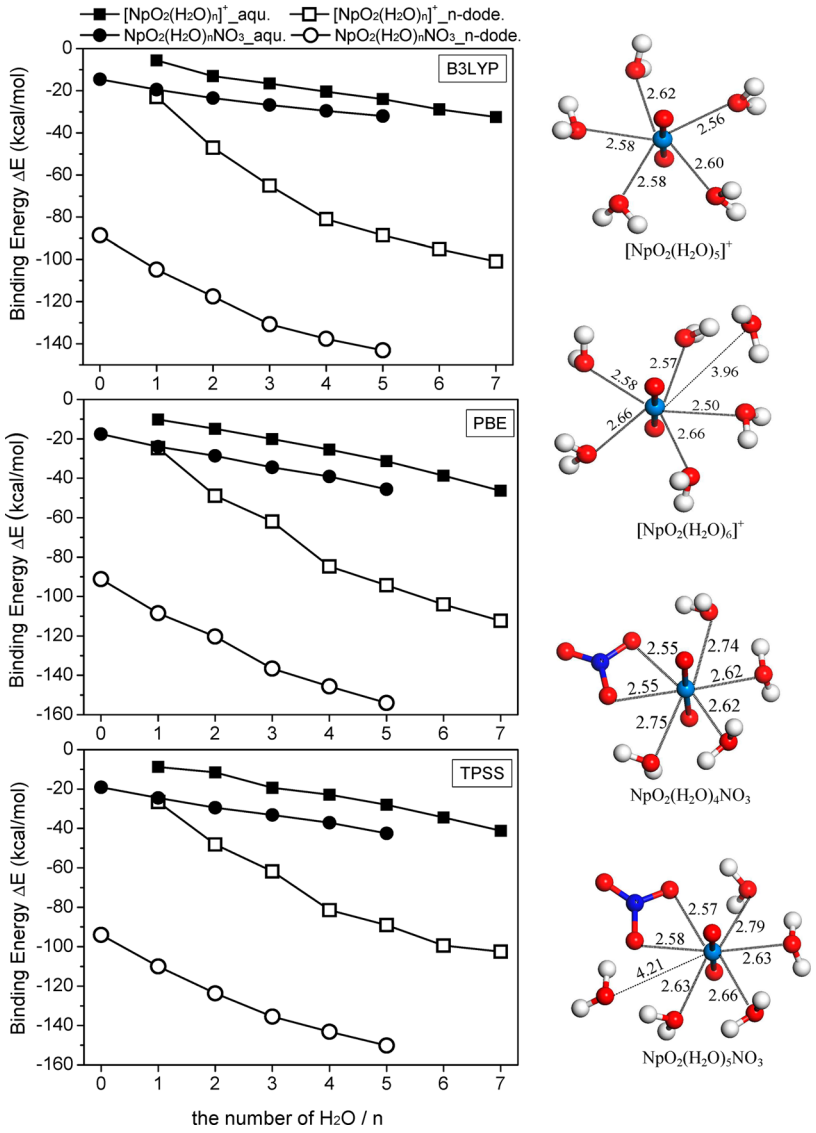

Figure 1. Binding energy ΔE (kcal/mol) of complexes $[NpO_2(H_2O)_n]^+$ and $NpO_2(H_2O)_nNO_3$ as a function of the number of coordinated water molecules, *n*, in aqueous (filled symbols) and organic *n*-dodecane (open symbols) phases calculated at the BS2 level utilizing B3LYP, PBE, and TPSS methods. The optimized geometries of $[NpO_2(H_2O)_n]^+$ and $NpO_2(H_2O)_nNO_3$ saturated with water molecules in the first coordination shell of Np^V are shown on the right-hand side with key geometrical parameters in angstroms. Color code: cyan, Np; red, O; blue, N; white, H.

dispersion correction was not included here. According to two recent comparative studies, both of which handle the coordination chemistry of heavy transition-metal elements, with one calculating the C−H activation energies by pincer complexes of late platinum group metals[80] and the other concerning the characterization of three uranium complexes,[81] the empirical dispersion correction according to Grimme et al.[82] was shown to have little effect on the barrier heights and relative energies.

To evaluate the solvent effect of polar water and apolar *n*-dodecane, all stationary points were reoptimized and confirmed to be energy minima by vibrational frequency calculations using the three functionals with the polarizable continuum model.[83] Single-point-energy calculations were then carried out to refine energies with the larger basis set 6-311++G(d,p) to describe the nonmetal atoms. This basis set is labeled as BS2. Note that, in the present work, spin−orbit coupling effects were not included.

Several analysis techniques were used to understand the bonding and electronic properties of the complexes. These include the AIM technique and the ELF according to Savin et al.[59] and Silvi and Savin,[60] with which the bonding and electronic properties of all complexes were characterized. The main properties of the (3, −1) BCP in the gradient field of the electron density were analyzed. For comparison, analysis of the natural localized molecular orbital (MO) was done to explore the chemical bonding between the molecular fragments. Charge decomposition analysis (CDA)[84,85] was performed to quantify the charge donation and back-donation between the metal and ligand fragments in complexes. The *Multiwfn* package[86] was used to carried out the above-mentioned analysis based on the optimized wave functions generated in the quantum-mechanical calculations.

3. RESULTS AND DISCUSSION

3.1. Structure and Thermochemical Stability. To determine the ability of neptunyl coordinated with the targeted ligands (L) in gas and solution phases, the structures and thermodynamic stability of complexes, including $[NpO_2(H_2O)_n]^+$ (n = 1−7), $NpO_2(H_2O)_nNO_3$ (n = 0−5), $[NpO_2L(H_2O)_n]^+$ (n = 0, 1), and NpO_2LNO_3, which may exist in the nitrate solution during the extraction process, were investigated.

Explicit Treatment of the First Solvation Shell of Neptunyl Complexes $[NpO_2(H_2O)_n]^+$ (n = 1−7) and $NpO_2(H_2O)_nNO_3$ (n = 0−5). In an aqueous solution, neptunyl exists in its hydrated forms via complexation with water molecules, and

dx.doi.org/10.1021/ic500138w | Inorg. Chem. 2014, 53, 7848−7860

experimental studies have suggested a coordination number ranging from 1 to 5 in its equatorial plane.[87−93] In the study of a ligand-exchange reaction, an implicit treatment of the solvation effect on a naked ion in a polar solvent may be insufficient to obtain an accurate estimation of the reaction energies. To evaluate the importance of an explicit treatment for the interaction between the water solvent and neptunyl in its first coordination shell, we have optimized a series of complexes with various numbers of water molecules and compared the stabilization energies, which are plotted in Figure 1 for complexes $[NpO_2(H_2O)_n]^+$ (n = 1−7) and $NpO_2(H_2O)_nNO_3$ (n = 0−5), as a function of the number of water molecules in aqueous and organic n-dodecane phases.

The binding energies of $[NpO_2(H_2O)_n]^+$ and $NpO_2(H_2O)_nNO_3$ show consistent tendencies using the three functionals in all media and indicate that water brings more stabilization to the complexes of neptunyl with water as the number of coordinated water molecules increases. In $[NpO_2(H_2O)_n]^+$ complexes, when the number of water molecules is up to 5, the coordination of $[NpO_2]^+$ with water tends to saturate in both media. The addition of more water molecules leads to the formation of intermolecular hydrogen bonds among water molecules, which brings further stabilization, while the incoming water molecule does not build a direct interaction with the Np atom but stays in the outer shell. As can be seen in Figure 1, the first coordination shell of NpO_2^+ can accommodate 5 water molecules at most, while the excess water in the $[NpO_2(H_2O)_6]^+$ complex is pushed away from the Np ion. The distance of the $Np-O_{water}$ in the $[NpO_2(H_2O)_5]^+$ complex ranges from 2.56 to 2.62 Å in the gas phase, from 2.53 to 2.62 Å in the aqueous solution, and from 2.55 to 2.62 Å in the n-dodecane solution. In $[NpO_2(H_2O)_n]^+$ (n > 5), the distances of the uncoordinated $Np-O_{water}$ are more than 3.70 Å independent of the media, which suggests a maximal coordination number of NpO_2^+ as 5, in agreement with previous studies.[89−93]

The presence of one nitrate ion does not change the trend of the binding energies; i.e., similar to that of $[NpO_2(H_2O)_n]^+$, for the neutral nitrated complexes $NpO_2(H_2O)_nNO_3$, it is stabilized via coordination with water as the number of water molecules increases from n = 0 to 5 and the coordination tends to be saturated at n = 4. This is also reflected by the geometry structures displayed in Figure 1, in which the maximum coordination number of neptunyl is 6 in the first coordination sphere, containing four water molecules and one bidentate nitrate ligand. In the $NpO_2(H_2O)_5NO_3$ complex, the distances of four $Np-O_{water}$ coordination bonds range from 2.57 to 2.79 Å in the gas phase (2.56−2.80 and 2.55−2.80 Å in the aqueous and n-dodecane solutions, respectively), while the fifth water molecule, which was delicately placed within the range of the dative bond interaction with Np in the starting structure, moved away from the metal center to a nonbonding distance longer than 4.20 Å during optimization. In Figure 1, it can also be seen that nitration of the complexes brings more stabilization compared to the hydrated neptunyls, which may be contributed by electrostatic interaction.

$[NpO_2L(H_2O)_n]^+$ (n = 0, 1) and NpO_2LNO_3 Complexes. To assess the complexation ability of bis(1,2,4-triazine-3-yl) N-donor ligands (L) with Np^V, the formations of $[NpO_2L]^+$, hydrated $[NpO_2LH_2O]^+$, and nitrated NpO_2LNO_3 complexes were investigated in gas and solution phases, where L denotes BTP, BTBP, and BTPhen and their C2- and $CyMe_4$-substituted analogues. As mentioned above, the neptunyl has a saturated coordination number of 5 in the absence of nitrate and 6 in the presence of nitrate, respectively. This implies that when coordinated to a tetradentate ligand L″, neptunyl is able to accommodate one water molecule or one NO_3^- ion molecule in its equatorial plane to saturate its first solvation shell, leading to a coordination number of 5 in $[NpO_2L''(H_2O)]^+$ and 6 in $NpO_2L''NO_3$, where the nitrate ion appears as a bidentate ligand (κ^2-O_2NO^-). Taking into account the other four coordination sites occupied by the N atoms of the tetradentate ligands, the geometry of $[NpO_2L''(H_2O)]^+$ can best be described as pentagonal-bipyramidal polyhedral and that of $NpO_2L''NO_3$ as hexagonal-bipyramidal polyhedral. The calculated bond distances between the central Np ion and the coordinated N and O atoms are listed in the Supporting Information (SI; Table S1) for all of the studied species.

As expected, the axial Np−O distances are elongated for all complexes. The Np−N(2) distance is shorter than that of Np−N(1) in all complexes, suggesting stronger interaction between Np and N(2) than between Np and N(1). The bond length r[Np−N(2)] and the difference (Δr) between r[Np−N(1)] and r[Np−N(2)] are illustrated in Figure 2. It is found that

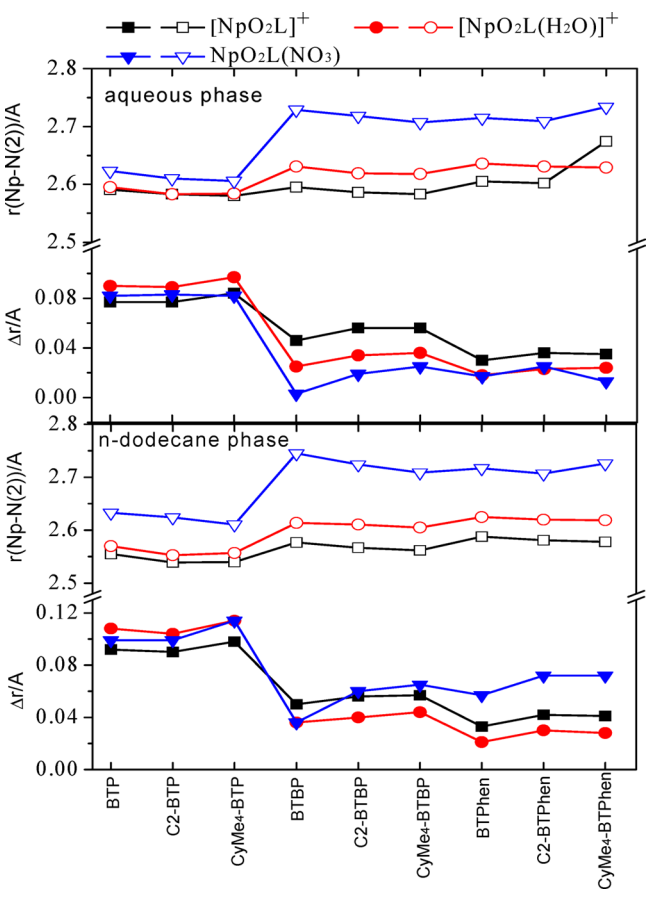

Figure 2. Calculated interaction distance r[Np−N(2)] (open symbol) and distance difference Δr (filled symbol) between r[Np−N(1)] and r[Np−N(2)] in the $[NpO_2L]^+$, $[NpO_2L(H_2O)]^+$, and $NpO_2L(NO_3)$ complexes in the aqueous (upper) and n-dodecane (bottom) phases. L represents BTP, BTBP, and BTPhen and their substituted analogues.

complexes display similar geometric tendencies independent of the type of media (gas, aqueous, and n-dodecane solution). The distances of Np−N(2) in the tetradentate L″ complexes are slightly longer than those in the tridentate L′ complexes. However, the differences (Δr) between r[Np−N(1)] and r[Np−N(2)] in the tetradentate L″ complexes are much smaller than those in the tridentate L′ complexes; i.e., the

dx.doi.org/10.1021/ic500138w | Inorg. Chem. 2014, 53, 7848−7860

tetradentate L″ complexes are more symmetric than the tridentate L′ complexes in view of their Np−N bond distances (ca. 0.04 and 0.10 Å for Δr in the tetradentate L″ and tridentate L′ complexes, respectively). This minor difference can be attributed to the distinct cavity sizes in the tetradentate and tridentate ligands and their electronic structures, as discussed later. Figure 2 also shows that substituents on the triazinyl rings have a minimal effect on the optimized metal−ligand bond lengths.

The binding energy of neptunyl chelated to ligands in the presence of water and NO_3^- in aqueous and organic phases is presented in Figure 3, which is calculated at the 6-311++G(d,p) level utilizing the B3LYP, PBE, and TPSS methods. All three functionals show the same tendency for the binding energy of neptunyl complexes. The following messages may be noted: (i) The overall trends of the binding energies for complexes $[NpO_2L]^+$ and $[NpO_2L(H_2O)]^+$ are similar to those of the distance difference Δr between r[Np−N(1)] and r[Np−N(2)] shown in Figure 2, and it may be deduced that the coordination strength in $[NpO_2L(H_2O)_n]^+$ (n = 0, 1) is correlated to the distance difference between Np−N(1) and Np−N(2) rather than to the shorter Np−N(2) bond length alone. Bis(1,2,4-triazine) N-donor ligands in which the bridging group is substituted by dipyridyl (L″ = BTBPs) or orthophenanthroline (L″ = BTPhens) have smaller Δr between Np−N(1) and Np−N(2) and appear with stronger chelating capability toward neptunyl than the corresponding pyridine substituents (L′ = BTPs). (ii) When the NO_3^- ion is coordinated to the Np^V center, a considerable increase of the binding energy is observed relative to that of complexes without NO_3^- in the organic phase, implying the importance of the presence of nitrate to stabilization of the neptunyl complexes in the organic phase. (iii) The C2-substituted complexes in all cases seem to display a stronger thermodynamic stability than the other analogues independent of the type of media, especially for complexation of C2-BTPhen with neptunyl.

3.2. Possible Ligand-Exchange Reaction Modes.

Extraction via phase separation is a complicated process, and it involves one or several ligand-exchange reactions during contact of the aqueous and organic phases, which may be an equilibrium or nonequilibrium process, and subsequent transfer of the complexes from the interface into the organic phase. To date, little information on the extraction reactions of Np^V has been obtained either in experimental or in theoretical studies. In order to identify the separation process in the case of neptunyl, three possible reaction modes were considered here and compared in terms of thermodynamics.

Mode A: competition of L against water, i.e., interaction of the hydrated neptunyl with organic ligands in the absence of the nitrate ion, according to eq 1.

$$[NpO_2(H_2O)_m]^+ + L \rightarrow [NpO_2L(H_2O)_n]^+ + (m - n)H_2O \quad (1)$$

Mode B: competition of L against water with nitrate bound; i.e., the hydrated neptunyl is nitrated first and then interacts with ligands, according to eq 2.

$$NpO_2(H_2O)_mNO_3 + L \rightarrow NpO_2LNO_3 + mH_2O \quad (2)$$

Mode C: competition of L against water assisted by the nitrate ion, i.e., interaction of the hydrated neptunyl with lipophilic ligands in the presence of the nitrate anion, according to eq 3.

$$[NpO_2(H_2O)_m]^+ + L + [NO_3]^- \rightarrow NpO_2LNO_3 + mH_2O \quad (3)$$

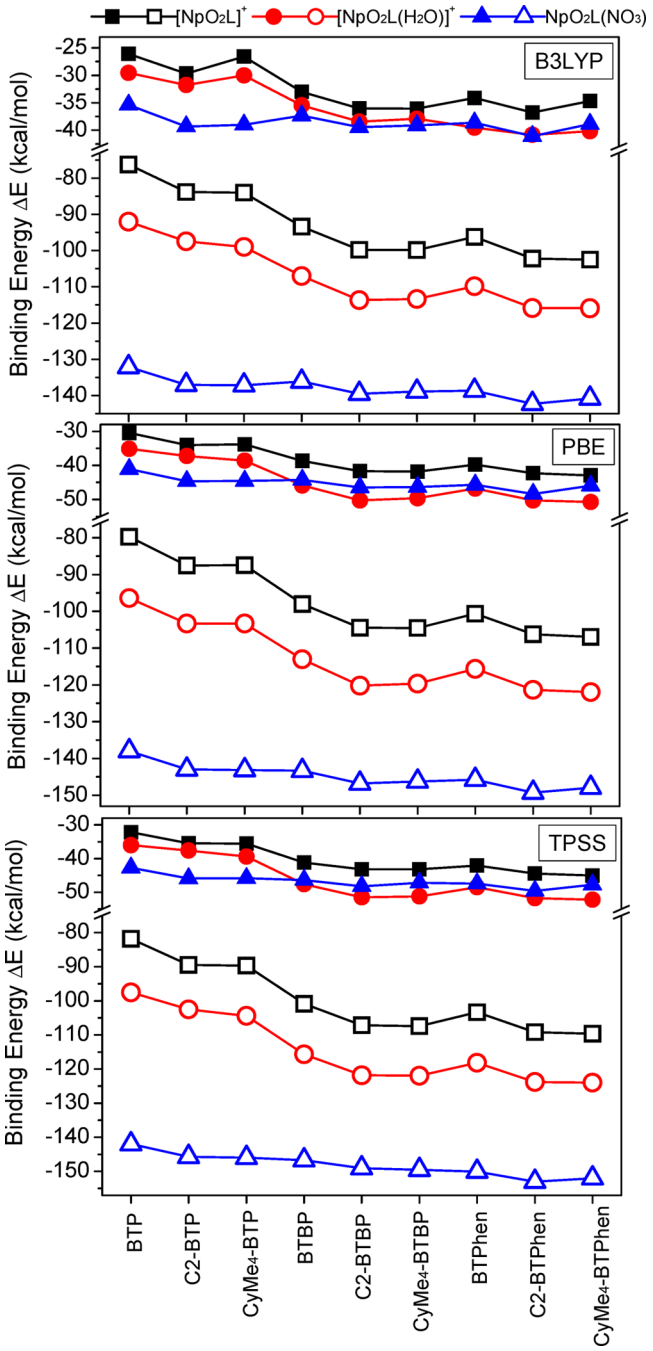

Figure 3. Calculated binding energy ΔE (kcal/mol) for the $[NpO_2L]^+$, $[NpO_2L(H_2O)]^+$, and $NpO_2L(NO_3)$ complexes in aqueous (filled symbols) and organic n-dodecane (open symbols) phases at the BS2 level utilizing the B3LYP, PBE, and TPSS methods, where L represents BTP, BTBP, and BTPhen and the respective substituted analogues.

Here, m and n are the optimal numbers of water molecules coordinated to neptunyl, as discussed above. The Gibbs free energy changes of these processes are tabulated in Table 1 for coordinatively saturated complexes, calculated at the B3LYP/BS1 level, as well as Tables S3 and S4 in the SI at the PBE and TPSS levels, respectively. (Table S2 in the SI concerns possible n and m corresponding to various reactions under unsaturated or saturated conditions.)

According to our calculations, all three functionals reach the same conclusion; i.e., mode B is endothermic or slightly

dx.doi.org/10.1021/ic500138w | Inorg. Chem. 2014, 53, 7848−7860

Table 1. Possible Ligand-Exchange Reactions Leading to the Formation of the Coordinatively Saturated Complexes $[NpO_2L(H_2O)_m]^+$ (m = 1, 2) and NpO_2LNO_3 at the B3LYP Level

reaction mode[a]		BTPs			BTBPs			BTPhens		
		C0[b]	C2	$CyMe_4$	C0	C2	$CyMe_4$	C0	C2	$CyMe_4$
mode A:[c] $[NpO_2(H_2O)_5]^+ + L \rightarrow [NpO_2L(H_2O)_m]^+ + nH_2O$	ΔG_r(aq)	−6.02	−3.95	−3.45	−10.98	−12.17	−9.41	−10.79	−11.48	−8.60
	ΔG_r(*n*-dodecane)	−10.60	−5.96	−12.17	−17.45	−20.08	−17.76	−18.57	−20.90	−18.83
	ΔG_r(part.)	17.07	12.42	15.86	2.82	0.19	2.51	1.69	−0.63	1.44
mode B: $NpO_2(H_2O)_4NO_3 + L \rightarrow NpO_2LNO_3 + 4H_2O$	ΔG_r(aq)	−4.56	−4.77	−2.01	−3.76	−3.51	−3.14	−3.26	−3.14	−1.51
	ΔG_r(*n*-dodecane)	5.59	3.64	6.59	4.27	4.46	7.47	3.45	3.08	7.78
	ΔG_r(part.)	6.78	4.83	7.78	5.46	5.65	8.66	4.64	4.27	8.97
mode C: $[NpO_2(H_2O)_5]^+ + L + NO_3^- \rightarrow NpO_2LNO_3 + 5H_2O$	ΔG_r(aq)	−13.99	−14.31	−11.55	−13.30	−13.05	−12.68	−12.80	−12.68	−11.04
	ΔG_r(*n*-dodecane)	−51.27	−53.21	−50.26	−52.59	−52.40	−49.51	−53.40	−53.78	−49.13
	ΔG_r(part.)	−2.76	−4.71	−1.76	−4.08	−3.89	−0.88	−4.90	−5.27	−0.57

[a] ΔG_r(aq) and ΔG_r(*n*-dodecane) refer to reaction Gibbs free energies (kcal/mol) in aqueous and organic phases calculated at the B3LYP/BS1 level, respectively. ΔG_r(part.) refers to partition Gibbs free energies (kcal/mol) at the interface between the aqueous and organic phases. (L = BTPs, BTBPs, and BTPhens inclusive of the respective substituents.) [b] C0 refers to unsubstituted ligands. [c] For L = BTPs, m = 2 and n = 3. For L = BTBPs and BTPhens, m = 1 and n = 4.

exothermic relative to other modes in three media, as shown in Tables 1 and S2−S4 in the SI. The other two modes are more exothermic in the gas, aqueous, and organic phases, suggesting a higher possibility for neptunyl to coordinate to the three families of ligands in a nitric acid free or diluted nitric acid environment. Especially, our calculation indicates that, in the diluted nitric acid solution, where the chelation reaction of the hydrated neptunyl with lipophilic ligands may proceed under the assistance of a nitrate anion, the ligand-exchange reactions with water replaced by one lipophilic ligand and one nitrate ion (mode C) display stronger exothermicity in all cases. In mode C, the reaction Gibbs free energies at the B3LYP level in the gas phase, aqueous solution, and organic *n*-dodecane solvent are in the ranges of ca. −115 to −90, −15 to −8, and −63 to −47 kcal/mol, respectively, whereas in the nitric acid free mode (mode A), they are ca. −44 to −10, −12 to −0.3, and −30 to 5 kcal/mol, respectively. These results suggest that the condition of diluted nitric acid favors complexation of neptunyl and the ligands, which are also supported by the results of the PBE and TPSS functionals (see Tables S3 and S4 in the SI).

In the two-phase systems with one aqueous phase, where the neptunyl ion is solved initially, and one organic phase, which carries an extractant compound, it is possible for the metal complexes to be formed at the interface and then extracted into the organic phase. Concerning the phase distribution change of each species that participates in the extraction process, the above-mentioned three modes may have the forms below:

Mode A:

$$[NpO_2(H_2O)_m]_{aq}^+ + L_{org} \rightarrow [NpO_2L(H_2O)_n]_{org}^+ + (m-n)H_2O_{aq} \quad (4)$$

Mode B:

$$[NpO_2(H_2O)_mNO_3]_{aq} + L_{org} \rightarrow [NpO_2LNO_3]_{org} + mH_2O_{aq} \quad (5)$$

Mode C:

$$[NpO_2(H_2O)_m]_{aq}^+ + L_{org} + [NO_3]_{aq}^- \rightarrow [NpO_2LNO_3]_{org} + mH_2O_{aq} \quad (6)$$

where the subscripts aq and org denote the species in aqueous and organic phases, respectively. The partition free energy ΔG_r(part.) is defined as the reaction Gibbs free energy change of the extraction process, which includes the Gibbs free energy change [ΔG_r(aq)] of the ligand-exchange reaction in an aqueous phase and that required to realize the transfer of the lipophilic ligand ($\Delta G_{L_{aq}\rightarrow L_{org}}$) and the newly formed complexes ($\Delta G_{[complex]_{aq}\rightarrow[complex]_{org}}$) from the aqueous to organic phase, according to the following thermodynamic cycle:

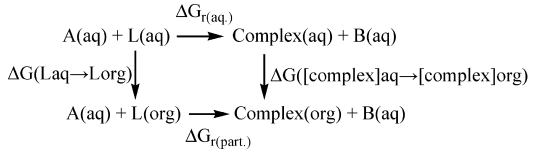

$$\Delta G_{r(part.)} = \Delta G_{r(aq.)} + \Delta G([complex]aq \rightarrow [complex]org) - \Delta G(Laq \rightarrow Lorg) \quad (7)$$

The partition Gibbs free energies ΔG_r(part.) of the three modes are plotted in Figure 4 and tabulated in Table 1 (as well as in Tables S2−S4 and Figure S1 in the SI). All three functionals give a similar picture; i.e., mode C is predicted to be more exothermic, suggesting a higher thermodynamic preference than modes A and B.

In addition, the number of coordinated water molecules in the hydrated neptunyl shows an influence on complexation. For the water → organic phase-transfer process, the saturated hydration states of the neptunyl ion bring more negative ΔG_r(part.) values (m = 5 and 6) than its unsaturated hydration states (m = 3 and 4; see Figure S1 and Table S2 in the SI), suggesting that the saturated hydration of the neptunyl ion favors the complexation reaction.

According to the reaction partition free energies [ΔG_r(part.)] from water to the organic phase and the reaction free energies [ΔG_r(*n*-dodecane)] in the organic solvent (see Tables 1 and S3 and S4 in the SI and Figure 4), C2-BTPhen and BTPhen show

dx.doi.org/10.1021/ic500138w | Inorg. Chem. 2014, 53, 7848−7860

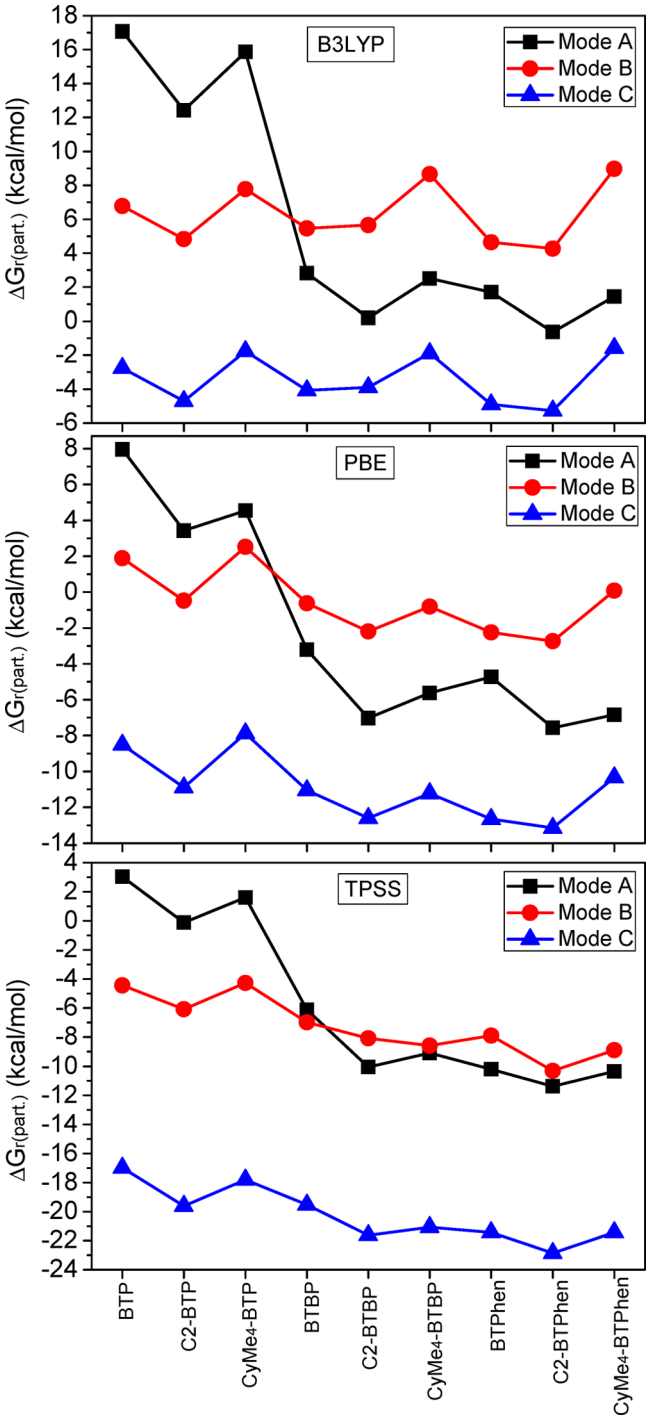

Figure 4. Partition Gibbs free energy ΔG_r(part.) (kcal/mol) at the interface between the aqueous and organic *n*-dodecane phases for the coordinatively saturated complexes of neptunyl in three reaction modes: mode A, $[NpO_2(H_2O)_m]^+ + L \rightarrow [NpO_2L(H_2O)_n]^+ + (m - n)H_2O$; mode B, $NpO_2(H_2O)_mNO_3 + L \rightarrow NpO_2LNO_3 + mH_2O$; mode C, $[NpO_2(H_2O)_m]^+ + L + [NO_3]^- \rightarrow NpO_2LNO_3 + mH_2O$.

the strongest complexation capability relative to other ligands, whereas the complexes of BTPs appear with the least complexation strength. This analysis makes it clear that the relative contribution of the central orthophenanthroline moiety is most pronounced compared to its pyridine counterparts, which is consistent with the complexing character of Am and Eu reported previously.[26,27,34] Furthermore, the complexation of neptunyl with the ligands studied here is found to feel the influence of the lateral alkyl substituents on the triazinyl rings. According to our calculations, the ligands with the ethyl group (C2) display stronger chelation ability in the reactions than the other ligands, which is in agreement with the thermodynamic stability discussed in the previous section. We note that the presence of $CyMe_4$ seems to not favor the complexation reactions; however, it is conceivable that the presence of such a bulky hydrophobic group may improve the solubility of the ligand, so does the complex, in the organic phase.

In order to further probe the influence of the substituents of ligands on complexation reactions, the deformation energy of the ligand required for complexation, which was defined as the energy difference between the ligand in the complex and the free ligand, was calculated at the B3LYP/6-311++G(d,p) level in aqueous and organic phases, as shown in Figure 5 as well as the correlation between the deformation energy and atomic positional root-mean-square deviation (RMSD) of all non-H "backbone" atoms of the ligands (Figure 5b). It can be seen (Figure 5b) that complexes formed with BTBPs require larger deformation of the ligands compared to the BTP cases with higher deformation energies. When the two pyridine rings are annulated as in the BTPhen family of ligands, the deformation of the ligands during complexation becomes small again compared to that of BTBP, which suggests an increase of the rigidity of the ligands due to annulation.

In view of the thermodynamics, in the aqueous phase, the deformation energies in the process $[NpO_2L(H_2O)]^+ \rightarrow NpO_2LNO_3$ decrease only in the cases of C2-BTPhen and BTPhen (Figure 5a), implying that for these two ligands the formation of NpO_2LNO_3 gains from the deformation of the ligands. The $CyMe_4$ substituent is observed to bring more deformation energy than the C2 substituent for all of three types of ligands in both the aqueous and organic phases. Especially, $CyMe_4$-BTPhen shows exceptional deformation in the process $[NpO_2L(H_2O)]^+ \rightarrow NpO_2LNO_3$ in both the aqueous and organic phases, suggesting the possibility of a very slow ligand-exchange reaction. This is because the rigid framework of the bridging group in $CyMe_4$-BTPhen makes it difficult to be out of shape. These results are in agreement with the above discussions and show that the deformation of the ligand may be one of the factors influencing complexation reactions.

3.3. Bonding Characteristics. *3.3.1. Electron Density Analysis.* Topology analysis was done to investigate the ionic/covalent nature of the metal−ligand interaction, which could not be readily derived from the orbital term. In the framework of the AIM theory, the electron density (ρ), its Laplacian ($\nabla^2\rho$), and the electronic energy density $[H(\mathbf{r})]$ at a BCP may provide information about the strength and characteristics of the bond. Large ρ values and the values of $\nabla^2\rho < 0$ and $H(\mathbf{r}) < 0$ refer to the shared interaction or covalent bond, while small ρ values and values of $\nabla^2\rho > 0$ and $H(\mathbf{r}) > 0$ are indicators of ionic or hydrogen bonds and van der Waals interactions.[42,43] Another quantitative indicator for covalency is the delocalization index (DI), which integrates the electron density in the bonding region between two atoms and can be used as a measure of the bond order.

B3LYP, PBE, and TPSS data were used to calculate the electron density in the equatorial plane of neptunyl complexes, including $[NpO_2L]^+$, $[NpO_2L(H_2O)]^+$, and $NpO_2L(NO_3)$ (L = BTP, BTBP, and BTPhen), as shown in Figure 6A−I and Table S6 in the SI, where pictorial representations of the

dx.doi.org/10.1021/ic500138w | Inorg. Chem. 2014, 53, 7848−7860

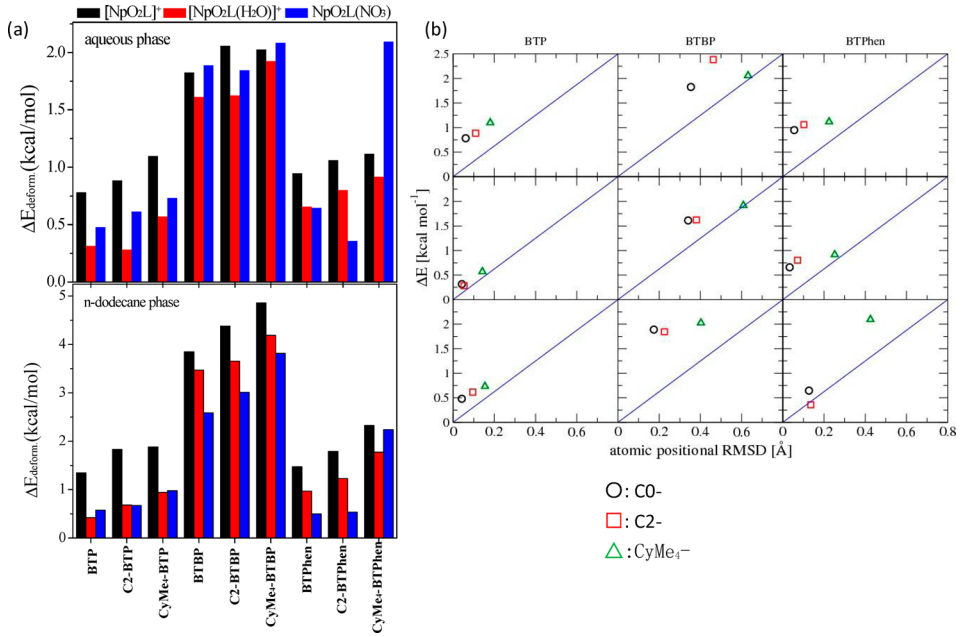

Figure 5. Deformation energies ΔE (kcal/mol) of ligands to form $[NpO_2L(H_2O)_n]^+$ (n = 0, 1) and NpO_2LNO_3 complexes (left, a) calculated at the B3LYP/6-311++G(d,p) level in aqueous (upper) and organic (lower) phases and correlation between the deformation energies and atomic positional RMSD in the aqueous phase (right, b). The non-H "backbone" atoms, i.e., the C and N atoms of the ring units, were used to calculate the RMSD. The first, second, and third rows refer to $[NpO_2L]^+$, $[NpO_2L(H_2O)]^+$, and NpO_2LNO_3 complexes, respectively, in part b.

electron density are given. The corresponding QTAIM topology analysis data for the Np−N and Np−O_{eq} BCPs in all complexes studied are summarized in the SI (Table S5), in which all indexes show the same trend as the electron density ρ. The electron density ρ, its Laplacian $\nabla^2\rho$, and the energy density H indicate that the Np−N bonds in all complexes are predominantly ionic, which is also supported by the ELF[58−60] and localized orbital locator[94] analysis.

It is noticed that the ρ_{BCP} values of the Np−N bonds in the family of BTP complexes are slightly larger than those in the BTBP and BTPhen complexes (0.038−0.051 and 0.029−0.045 e^-/bohr^3 for the BTP and BTBP/BTPhen complexes, respectively), suggesting a stronger covalency of the Np−N bond in the BTP complexes than in the BTBP and BTPhen complexes. In addition, the larger ρ_{BCP} values of the Np−N(2) bonds in the BTP complexes indicate their higher covalency than the Np−N(1) bonds, consistent with the geometric parameters. In contrast, for the families of the BTBP and BTPhen complexes, the ρ_{BCP} values of the Np−N(1) and Np−N(2) bonds are close to each other (see Figure 6), suggesting more electron delocalization in the interaction of Np with these two types of tetradentate ligands compared to the analogous BTP complexes. This shows that the trend of the electron density difference between the Np−N(1) and Np−N(2) bonds is similar to that of the geometrical parameters Δr (r[Np−N(1)] − r[Np−N(2)]) as well as that of the binding energies. These descriptions can also be supported by data obtained from two other functionals (see Table S6 in the SI). Accordingly, it can be deduced that, in the case of neptunyl coordination with bis(1,2,4-triazine) N-donor ligands, electron delocalization in the Np−N bonds can enhance the stability of the complexes.

Upon comparison of the electron density of the Np−O_{eq} bonds with that of the Np−N bonds in all cases, it is noteworthy that the ρ_{BCP} values of the Np−O_{eq} bonds are larger (see Figure 6 and Tables S5 and S6 in the SI), especially for Np−O_{eq} bonds in nitrated neptunyl complexes. Their ionic characterisitics are still strong but with a larger degree of covalency, as confirmed by the values of DI as well, which are in the ranges of 0.862−0.923 and 0.902−0.977 for the Np−O_{eq} bonds in $[NpO_2L(H_2O)]^+$ and $NpO_2L(NO_3)$, respectively. Obviously, the Np−O_{eq} coordination bonds cause an increase in the covalent contribution to the stability of the hydrated or nitrated neptunyl complexes.

3.3.2. Charge Transfer in the Complexes. The CDA[84] and extended charge decomposition analysis (ECDA)[85] methods are used to probe how charges are transferred between metal and ligand fragments in targeted complexes to achieve charge equilibrium. The idea of CDA is to quantify the charge donation and back-donation between the metal fragment and ligands in the complexes based on fragment orbitals. The difference between the total number of donation and back-donation electrons may be regarded as the net transferred electrons. The most remarkable feature of CDA is that electron transfer can be decomposed to the contribution of complex orbitals. ECDA takes into account the electron polarization effect (PL) in addition to the charge-transfer effect (CT), and the transferred charge can be obtained according to CT(A→B) − CT(B→A) = [PL(A) + CT(A→B)] − [PL(A) + CT(B→A)]. It reveals how many electrons are transferred between the two fragments A and B.

Table 2 (as well as Tables S7 and S8 in the SI) lists the amount of the net charge transfer from the ligands to neptunyl in $[NpO_2L]^+$, $[NpO_2L(H_2O)]^+$, and $NpO_2L(NO_3)$ complexes by the CDA and ECDA methods. The net charge transfer from the ligands to neptunyl in the analogous complexes decreases in the order of $NpO_2L(NO_3)$ > $[NpO_2L(H_2O)]^+$ > $[NpO_2L]^+$ (in the ranges of 0.652−0.730, 0.550−0.679, and 0.447−0.567 e^- obtained by ECDA, respectively), which is in good agreement with their relative stabilities. Obviously, this charge-transfer order is consistent with the order of the electron-donating ligands, i.e., L + NO_3^- > L + H_2O > L. In $NpO_2L(NO_3)$ complexes, NO_3^- can easily access positively charged neptunyl

dx.doi.org/10.1021/ic500138w | Inorg. Chem. 2014, 53, 7848−7860

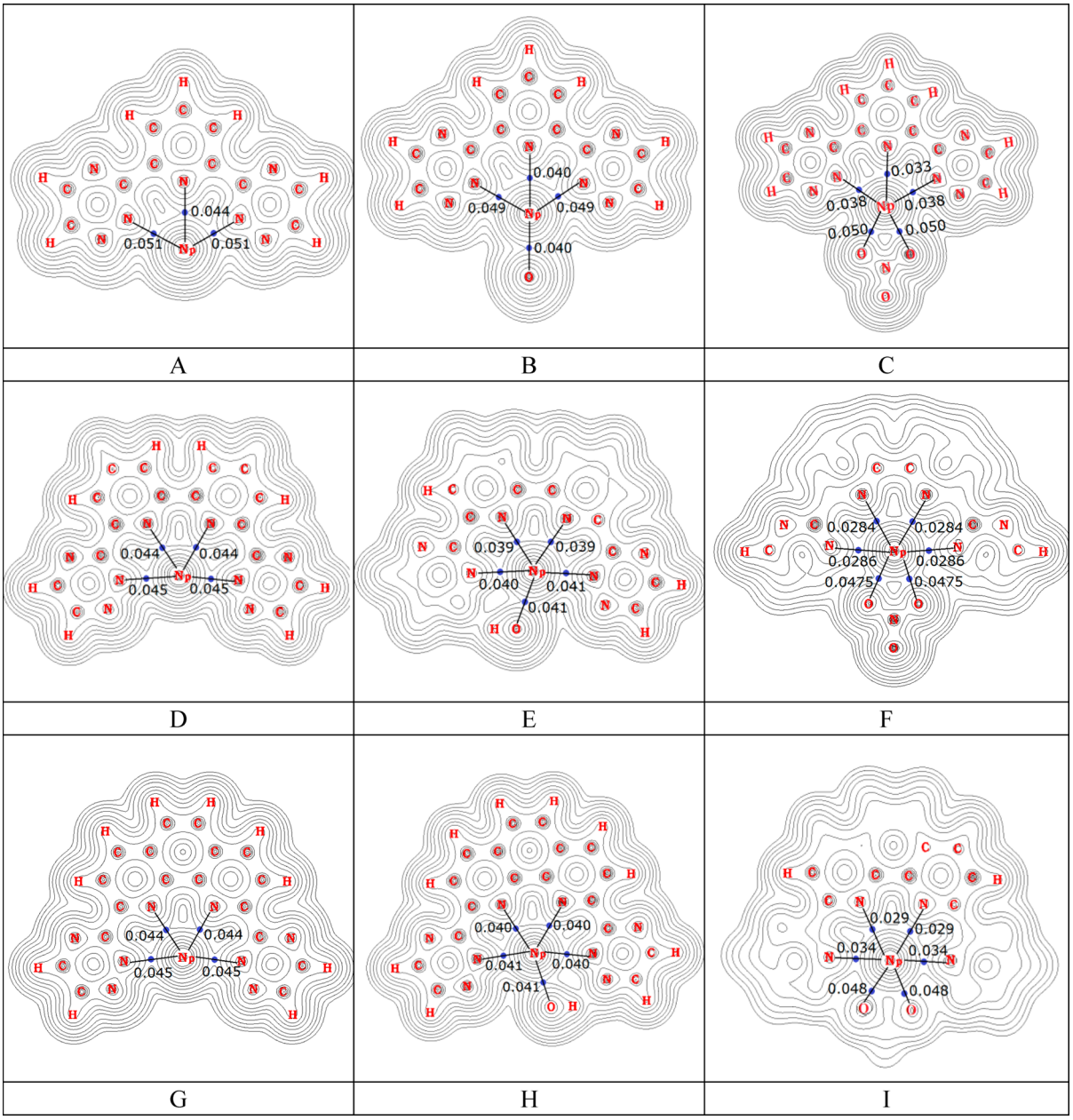

Figure 6. Contour maps of the electron densities in the equatorial plane of (A) $[NpO_2(BTP)]^+$, (B) $[NpO_2(BTP)(H_2O)]^+$, (C) $NpO_2(BTP)(NO_3)$, (D) $[NpO_2(BTBP)]^+$, (E) $[NpO_2(BTBP)(H_2O)]^+$, (F) $NpO_2(BTBP)(NO_3)$, (G) $[NpO_2(BTPhen)]^+$, (H) $[NpO_2(BTPhen)(H_2O)]^+$, and (I) $NpO_2(BTPhen)(NO_3)$. The equatorial plane is defined by the plane of the coordinated organic ligand. The BCPs are shown as small blue dots on the bond, and the values of the electron density (in $e^-/bohr^3$) at the BCPs are shown as well.

via electrostatic interaction and coordinate to the Np atom. It can be noticed charge-transfer analysis is also independent of the methods.

Upon comparison of NpO_2LNO_3 with $[NpO_2L(H_2O)]^+$ complexes, larger charge transfer is observed in NpO_2LNO_3 from NO_3^- to neptunyl, indicating a higher degree of covalency in the Np−O_{eq} bonds of NpO_2LNO_3 compared to the Np−O_{eq} bond of $[NpO_2L(H_2O)]^+$. This was also supported by the electron density ρ_{BCP}, which is larger in the Np−O_{eq} bonds of NpO_2LNO_3 complexes than those of $[NpO_2L(H_2O)]^+$ complexes, as shown in Figure 6. Consequently, although the ρ_{BCP} values of the Np−N bonds in the NpO_2LNO_3 complexes decrease because of the involvement of NO_3^- in electrostatic interaction, relatively large Np−O_{eq} ρ_{BCP} values, and more charge transfer to neptunyl, suffice to compensate for the decrease of the Np−N bonds covalency and result in an increase in the overall stability of the NpO_2LNO_3 complexes.

Charge transfers from the ligands to neptunyl in the family of tridentate BTP complexes were found to be lower compared to the tetradentate L″ complexes (Tables 2 and S7 and S8 in the SI). In connection with the lower stabilities of the BTP complexes than those of the BTBP and BTPhen complexes and the stronger Np−N covalency in the BTP complexes, it seems that charge transfer plays a more important role than the covalency of the Np−N bonds in the formation of these complexes, maybe resulting from quite feeble covalent characteristics in the neptunyl complexes. Meanwhile, the ligands with C2 and $CyMe_4$ substituents have larger charge transfer than their unsubstituted analogues. These results indicate that charge transfer from the ligands to neptunyl may

dx.doi.org/10.1021/ic500138w | Inorg. Chem. 2014, 53, 7848−7860

Table 2. Charge Transfer (e^-) in the $[NpO_2L(H_2O)_n]^+$ (n = 0, 1) and NpO_2LNO_3 Complexes from the Ligands to Neptunyl from CDA and ECDA, Calculated at the B3LYP Level[a]

	$[NpO_2L]^+$		$[NpO_2L(H_2O)]^+$		$NpO_2L(NO_3)$	
	$L \rightarrow NpO_2^+$		$L + H_2O \rightarrow NpO_2^+$		$L + NO_3^- \rightarrow NpO_2^+$	
L	CDA	ECDA	CDA	ECDA	CDA	ECDA
BTP	0.264	0.447	0.340	0.550	0.411	0.652
C2-BTP	0.289	0.493	0.361	0.587	0.431	0.680
$CyMe_4$-BTP	0.293	0.500	0.366	0.592	0.426	0.681
BTBP	0.314	0.520	0.398	0.633	0.440	0.717
C2-BTBP	**0.334**	**0.564**	**0.417**	**0.671**	**0.444**	**0.730**
$CyMe_4$-BTBP	**0.334**	**0.567**	**0.420**	**0.679**	0.439	**0.726**
BTPhen	0.308	0.519	0.395	0.628	0.439	0.705
C2-BTPhen	**0.336**	**0.561**	**0.417**	**0.665**	**0.443**	**0.730**
$CyMe_4$-BTPhen	**0.336**	**0.563**	**0.420**	**0.673**	0.437	0.714

[a]Bold font means a relatively large amount of charge transfer.

be a predominant factor for thermodynamic stability in the case of neptunyl coordinating with bis(1,2,4-triazine) N-donor ligands, and the presence of an electron-donating group such as C2 and $CyMe_4$ on the lateral triazinyl may enhance the charge transfer from ligand to metal, resulting in increasing stability with respect to unsubstituted complexes.

3.3.3. NAO Analysis. The NAO approach[61] was used to explore the nature of the Np−ligand coordination interaction. With this approach, the atomic orbital compositions of MOs were obtained and analyzed on how the 5f and 6d orbitals of Np contribute to the covalency.

Figure 7 shows the frontier valence MO diagram with the largest contribution to the Np−ligand bonds for complexes $[NpO_2L]^+$, $[NpO_2L(H_2O)]^+$, and $NpO_2L(NO_3)$ (L = BTBP as the representative), in which the two highest occupied α-spin orbitals accommodate the two unpaired 5f electrons of Np^V (SOMO and SOMO−1), similar to the situation of an U^{IV} center.[29] Table 3 presents the specific atomic orbital contributions to the corresponding MOs of three complexes shown in Figure 7 (as well as Tables S9 and S10 in the SI obtained from the PBE and TPSS data for the largest atomic orbital contributions).

Inspection of the frontier MOs (Figure 7) reveals a distinct orbital interaction between the Np and ligand atoms. In the $[NpO_2(BTBP)]^+$ complex, the second highest occupied MO (HOMO−1) is composed largely of the 5f orbital of Np and

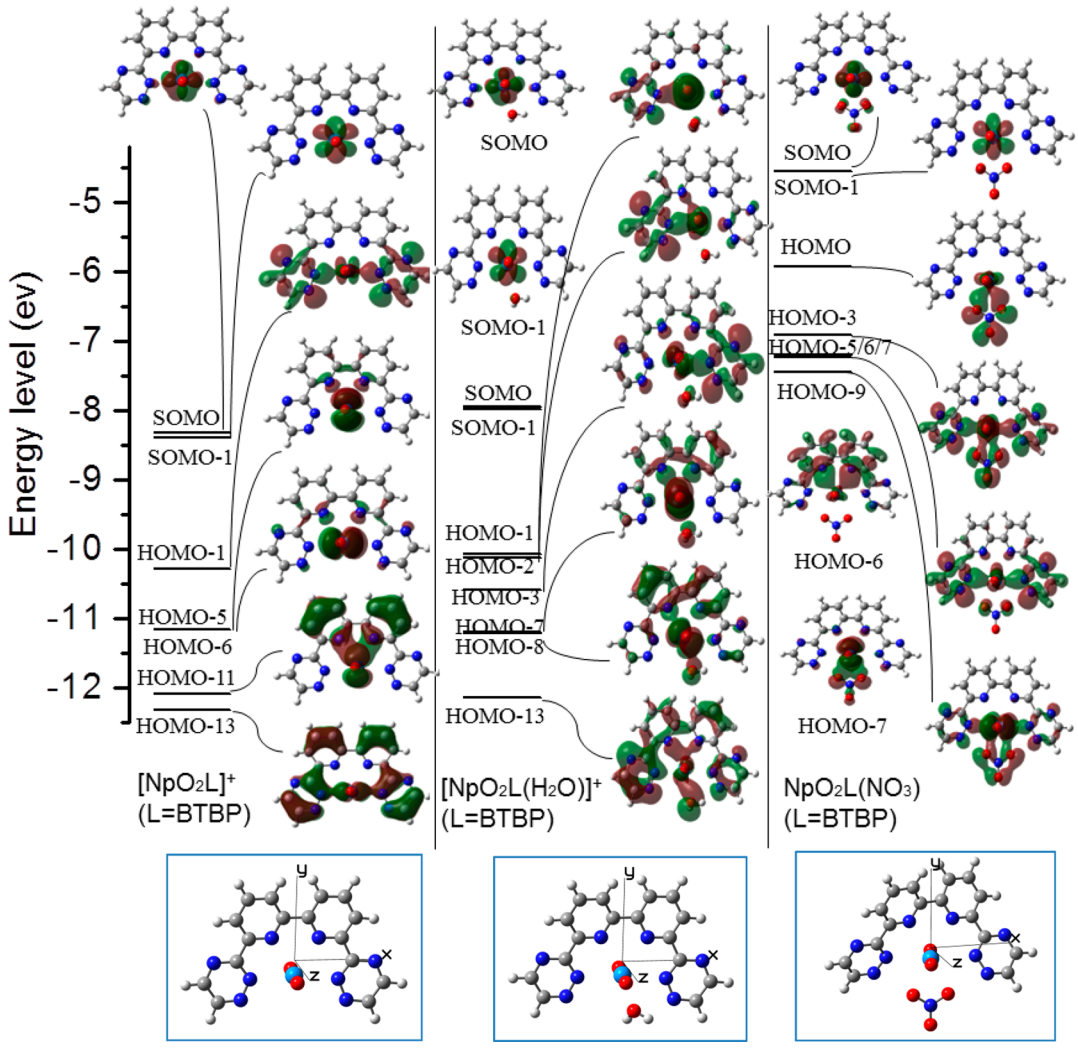

Figure 7. Representative α-spin MOs, including SOMO/SOMO−1 and valence MOs mixing between metal and ligand moieties in the complexes $[NpO_2L]^+$, $[NpO_2L(H_2O)]^+$, and $NpO_2L(NO_3)$. The corresponding contributions of metal and ligand atoms are listed in Table 3. The direction of the Cartesian axis is defined at the bottom. The isosurface value of the three-dimensional representations is set as 0.02 for all cases.

dx.doi.org/10.1021/ic500138w | Inorg. Chem. 2014, 53, 7848−7860

Table 3. Contributions (%) of Metal and Ligand Atoms to Representative MOs in Figure 7 for the Complexes $[NpO_2L]^+$, $[NpO_2L(H_2O)]^+$, and $NpO_2L(NO_3)$ (L = BTBP) at the B3LYP Level

$[NpO_2L]^+$	HOMO−1	HOMO−5	HOMO−6	HOMO−11	HOMO−13
Np	5.6	25.2	25.7	9.4	3.3
5f/6d	$5f_{x(x^2-3y^2)}$: 2.5 $5f_{z^3}$: 1.1	$5f_{yz^2}$: 21.3	$5f_{xz^2}$: 21.7	$6d_{yz}$: 8.9	$6d_{xz}$: 3.2
N(1)/N(2)	N(2): 21.3 ($2p_x$)	N(1): 4.1 ($2p_y$)	N(1): 3.1 ($2p_y$)	N(1): 10.3 ($2p_z$)	N(2): 3.7 ($2p_z$)

$[NpO_2L(H_2O)]^+$	HOMO−1	HOMO−2	HOMO−3	HOMO−7	HOMO−8	HOMO−13
Np	49.2	8.4	5.1	5.7	7.0	3.6
5f/6d	$5f_{z^3}$: 39.1	$5f_{z^3}$: 4.7	$5f_{yz^2}$: 1.2	$6d_{yz}$: 2.9	$6d_{xz}$: 3.1 $6d_{yz}$: 2.0	$6d_{yz}$: 1.7
		$5f_{x(x^2-3y^2)}$: 1.2	$6d_{x^2-y^2}$: 1.1		$5f_{yz^2}$: 1.2	
N(1)/N(2)	N(2): 2.1 ($2p_x$)	N(2): 16.6 ($2p_x$)	N(2): 13.0 ($2p_x$)	N(1): 1.5($2p_y$)	N(1): 3.7 ($2p_z$)	N(1): 4.0 ($2p_y$)
O (of H_2O)				3.7 ($2p_y$); 1.1 ($2p_z$)	2.2 ($2p_y$); 1.0 ($2p_z$)	22.5 ($2p_y$); 5.4 ($2p_z$)

$NpO_2L(NO_3)$	HOMO	HOMO−3	HOMO−5	HOMO−6	HOMO−7	HOMO−9
Np	5.4	7.5	2.3	5.5	21.8	23.4
5f/6d	$5f_{x(x^2-3y^2)}$: 2.7	$5f_{z^3}$: 2.9 $5f_{xz^2}$: 1.4	$6d_{x^2y^2}$: 1.3	$5f_{x(x^2-3y^2)}$: 1.4	$5f_{yz^2}$: 12.8	$5f_{xz^2}$: 12.1
	$6d_{xy}$: 1.3	$5f_{x(x^2-3y^2)}$: 1.3		$6d_{xy}$: 2.8	$5f_{z(x^2-y^2)}$: 4.2	$5f_{xyz}$: 3.0
N(1)/N(2)		N(2): 5.7 ($2p_x$)	N(2): 7.1 ($2p_x$)	N(1):19.5 ($2p_y$)		N(2): 1.1 ($2p_x$)
O (of NO_3)	19.3 ($2p_y$)	3.7 ($2p_x$)	2.3 ($2p_z$)		6.3 ($2p_y$); 1.8 ($2p_z$)	4.0 ($2p_x$)

the $2p_x$ orbital of N(2) in BTBP, in which the $5f_{x(x^2-3y^2)}$ and $5f_{z^3}$ atomic orbitals of Np have 3.6% contribution to HOMO−1 (Table 3). Degenerated HOMO−5 and HOMO−6 mainly consist of the 5f atomic orbital (21%) of Np and the $2p_y$ orbital of N(1) (3−4%), while HOMO−11 and HOMO−13 show interaction between the 6d orbital of Np and the $2p_z$ orbitals of N(1) and N(2), respectively.

In the hydrated complex $[NpO_2(BTBP)(H_2O)]^+$, the three frontier MOs, HOMO−1, HOMO−2, and HOMO−3, reveal the primary coordination sites of metal Np with N(2) atoms, in which the 5f orbital of Np has significant contribution to HOMO−1 and HOMO−2, whereas HOMO−3 has an admixture from the metal's 6d and 5f orbitals. The lower-lying occupied MOs, HOMO−7, HOMO−8, and HOMO−13, contain orbital overlap between the 6d orbitals of Np and the 2p orbitals of O_{eq} and N(1). In the nitrated complex $NpO_2(BTBP)(NO_3)$, the highest occupied MO (HOMO) is largely contributed by the NO_3^- moiety with significant contribution from a mixture of 5f and 6d orbitals of Np. Moreover, there is major 5f contribution of metal Np to the lower-lying MOs (HOMO−7 and HOMO−9) to form the corresponding Np−O_{eq} and Np−N coordination bonds.

Analysis of the MO diagrams (not shown) for the BTP and BTPhen target systems reveals an electronic structure similar to that of the analogous BTBP complexes; i.e., there is not only the metal d-based covalency but also significant participation of the metal 5f orbitals in the Np−ligand bonds in all cases as well. Notably, in the nitrated complexes, the donation of 5f (Np) orbitals to the Np−ligand bonds can be extended to the lower-lying occupied MOs [e.g., the contribution of 5f orbitals to HOMO−9 is still essential for the complexation of Np−ligand in the nitrated complex $NpO_2(BTBP)(NO_3)$]. This evidence is also manifestly reflected from PBE and TPSS functionals (see Tables S9 and S10 in the SI), which suggests a greater degree of covalence in the Np−ligand bonds or a factor of more charge transfer from ligand to metal occurring in the nitrated neptunyl complexes.

4. CONCLUSIONS

We presented a computational study on the complexation of neptunyl with three types of bis(1,2,4-triazine) N-donor extractants (BTPs, BTBPs, and BTPhens), which differ in their bridging groups, by using three DFT functionals, i.e., B3LYP, PBE, and TPSS, to evaluate their ability toward complexation with a neptunyl ion. By analysis of the geometry, electronic structures of the complexes, and thermodynamics of the complexation reactions, consistent conclusions are obtained from the calculations and are given as follows:

(1) QTAIM analysis shows that the metal−ligand interaction in all complexes studied are highly ionic. As expected, the coordination ability of Np with N(2) is stronger than that with N(1) in all targeted systems in view of the bond length and AIM topological analysis. The tendency of binding energies of the complexes is similar to that of the distance difference (Δr) between r[Np−N(1)] and r[Np−N(2)] but opposite to that of r[Np−N(2)], suggesting that electron delocalization, instead of the shorter r[Np−N(2)] alone, may influence the thermodynamical stability of the complexes. This is supported by the electron density analysis.

(2) According to CDA analysis, charge transfer from the ligand to Np decreases in the order of NpO_2LNO_3 > $[NpO_2L(H_2O)]^+$ > $[NpO_2L]^+$, which is the same as the order of the thermodynamic stability. It can be speculated that the extent of metal−ligand covalency, electron delocalization, and charge transfer in complexes plays a cooperative role for the stability of the complexes. When bis(1,2,4-triazine) N-donor ligands vary from tridentate BTPs to tetradentate BTBPs and BTPhens via alteration of the bridging group, electron delocalization and charge transfer increasingly become the main reason responsible for the coordination of L to neptunyl. Especially, coordinations of $[NpO_2]^+$ to tetradentate C2-BTPhen and C2-BTBP appear more favorable in all complexes because of electron delocalization and larger charge transfer. The presence of nitrate ions brings further stabilization to the complexes, taking advantage of maximum charge transfer and the greater degree of covalence in the Np−κ^2-O_2NO bond,

dx.doi.org/10.1021/ic500138w | Inorg. Chem. 2014, 53, 7848−7860

although the interaction between Np and L in NpO_2LNO_3 complexes is weakened.

(3) The detailed natural orbital analysis reveals that the Np−ligand bonding interactions in these complexes contain the 5f-based components in the frontier occupied MOs, implying participation of the 5f orbital in covalency interaction. Especially, in the nitrated complexes, 5f (Np) orbitals interact with the ligand with an extensive behavior in the lower-lying occupied MOs.

(4) The ligand-exchange reaction assisted by a nitrate ion, i.e., $[NpO_2(H_2O)_m]^+ + L + [NO_3]^- \rightarrow NpO_2LNO_3 + mH_2O$, is considered as the feasible reaction process in a dilute nitric acid solution in view of the thermodynamics for all targeted ligands. Its potential dominance is supported by the two-step extraction model in the aqueous−organic phase interface. In view of the reaction partition free energies $[\Delta G_r(\text{part.})]$ from water to an organic phase and the reaction formation free energies $[\Delta G_r(\text{n-dodecane})]$ in the organic solvent, the complexation of C2-BTPhen and BTPhen to neptunyl is the most favorable. It may be because C2-BTPhen and BTPhen combine the least deformation energies during the complexation and strong complexation stability in all complexes, leading to their higher propensity to coordinate with neptunyl than the other ligands.

■ ASSOCIATED CONTENT

Supporting Information

Additional information on the optimized structures, geometry parameters, and reaction energies in various reaction models, topology analysis, and atomic orbital composition in MOs obtained from PBE and TPSS functionals. This material is available free of charge via the Internet at http://pubs.acs.org.

■ AUTHOR INFORMATION

Corresponding Author

*E-mail: dwang@ihep.ac.cn.

Notes

The authors declare no competing financial interest.

■ ACKNOWLEDGMENTS

This work was financially supported by the National Natural Science Foundation of China (Grant 91026000 to Z.C., Grant 91126016 to S.D., Grant 21271132 to S.L., and Grant 91226105 to D.W.) and by the Chinese Academy of Sciences in the framework of a Frontier of Novelty program (Grants Y1515540U1 and Y2291810S3 to D.W.), which are gratefully acknowledged. Calculations were done on the computational grids in the computer center of the Institute of High Energy Physics, maintained by Drs. Jingyan Shi and Bowen Kan, in the Supercomputing Center of Chinese Academy of Sciences and in the National Supercomputing Center in Tianjin.

■ REFERENCES

(1) Dozol, M.; Hagemann, R. *Pure Appl. Chem.* **1993**, *65*, 1081.
(2) Nitsche, H.; Lee, S. C.; Gatti, R. C. *J. Radioanal. Nucl. Chem.* **1988**, *124*, 171.
(3) Kaszuba, J. P.; Runde, W. H. *Environ. Sci. Technol.* **1999**, *33*, 4427.
(4) Triay, I. R.; Robinson, B. A.; Mitchell, A. J.; Overly, C. M.; Lopez, R. M. *Mater. Res. Soc. Symp. Proc.* **1993**, *294*, 797.
(5) Capdevila, H.; Vitorge, P. *Radiochim. Acta* **1995**, *68*, 5.
(6) Prosser, S.; Popplewell, D.; Lloyd, N. *J. Environ. Radioact.* **1994**, *23*, 123.
(7) Balasubramanian, K.; Cao, Z. *Inorg. Chem.* **2007**, *46*, 10510.
(8) Clark, D.; Conradson, S.; Ekberg, S.; Hess, N.; Janecky, D.; Neu, M.; Palmer, P.; Tait, C. *New J. Chem.* **1996**, *20*, 211.
(9) Clark, D. L.; Conradson, S. D.; Ekberg, S. A.; Hess, N. J.; Neu, M. P.; Palmer, P. D.; Runde, W.; Tait, C. D. *J. Am. Chem. Soc.* **1996**, *118*, 2089.
(10) Clark, D. L.; Hobart, D. E.; Neu, M. P. *Chem. Rev.* **1995**, *95*, 25.
(11) Clark, D. L.; Conradson, S. D.; Neu, M. P.; Palmer, P. D.; Runde, W.; Tait, C. D. *J. Am. Chem. Soc.* **1997**, *119*, 5259.
(12) Gagliardi, L.; Roos, B. O. *Inorg. Chem.* **2002**, *41*, 1315.
(13) Hennig, C.; Ikeda-Ohno, A.; Tsushima, S.; Scheinost, A. C. *Inorg. Chem.* **2009**, *48*, 5350.
(14) Ikeda-Ohno, A.; Tsushima, S.; Takao, K.; Rossberg, A.; Funke, H.; Scheinost, A. C.; Bernhard, G.; Yaita, T.; Hennig, C. *Inorg. Chem.* **2009**, *48*, 11779.
(15) Kato, Y.; Kimura, T.; Yoshida, Z.; Nitani, N. *Radiochim. Acta* **1998**, *82*, 63.
(16) Kitamura, A.; Kohara, Y. *Radiochim. Acta* **2004**, *92*, 583.
(17) Xia, Y.; Rao, L.; Rai, D.; Felmy, R. *Radiochim. Acta* **1999**, *86*, 33.
(18) Benay, G.; Schurhammer, R.; Desaphy, J.; Wipff, G. *New J. Chem.* **2011**, *35*, 184.
(19) Benay, G.; Schurhammer, R.; Wipff, G. *Phys. Chem. Chem. Phys.* **2010**, *12*, 11089.
(20) Denecke, M. A.; Rossberg, A.; Panak, P. J.; Weigl, M.; Schimmelpfennig, B.; Geist, A. *Inorg. Chem.* **2005**, *44*, 8418.
(21) Drew, M. G.; Guillaneux, D.; Hudson, M. J.; Iveson, P. B.; Russell, M. L.; Madic, C. *Inorg. Chem. Commun.* **2001**, *4*, 12.
(22) Foreman, M. R.; Hudson, M. J.; Drew, M. G.; Hill, C.; Madic, C. *Dalton Trans.* **2006**, 1645.
(23) Guillaumont, D. *J. Phys. Chem. A* **2004**, *108*, 6893.
(24) Miguirditchian, M.; Guillaneux, D.; Guillaumont, D.; Moisy, P.; Madic, C.; Jensen, M. P.; Nash, K. L. *Inorg. Chem.* **2005**, *44*, 1404.
(25) Lewis, F. W.; Harwood, L. M.; Hudson, M. J.; Drew, M. G. B.; Modolo, G.; Syupla, M.; Desreux, J. F.; Bouslimani, N.; Vidick, G. *Dalton Trans.* **2010**, *39*, 5172.
(26) Hudson, M. J.; Harwood, L. M.; Laventine, D. M.; Lewis, F. W. *Inorg. Chem.* **2013**, *52*, 3414.
(27) Lewis, F. W.; Harwood, L. M.; Hudson, M. J.; Drew, M. G. B.; Desreux, J. F.; Vidick, G.; Bouslimani, N.; Modolo, G.; Wilden, A.; Sypula, M.; Vu, T.-H.; Simonin, J.-P. *J. Am. Chem. Soc.* **2011**, *133*, 13093.
(28) Drew, M. G. B.; Foreman, M. R. S.; Hudson, M. J.; Madic, C. *Inorg. Chem. Commun.* **2005**, *8*, 239.
(29) Foreman, M. R. S. J.; Hudson, M. J.; Geist, A.; Madic, C.; Weigl, M. *Solvent Extr. Ion Exch.* **2005**, *23*, 645.
(30) Geist, A.; Hill, C.; Modolo, G.; Foreman, M. R. S. J.; Weigl, M.; Gompper, K.; Hudson, M. J. *Solvent Extr. Ion Exch.* **2006**, *24*, 463.
(31) Kolarik, Z.; Mullich, U.; Gassner, F. *Solvent Extr. Ion Exch.* **1999**, *17*, 1155.
(32) Kolarik, Z.; Müllich, U.; Gassner, F. *Solvent Extr. Ion Exch.* **1999**, *17*, 23.
(33) Trumm, S.; Geist, A.; Panak, P. J.; Fanghänel, T. *Solvent Extr. Ion Exch.* **2011**, *29*, 213.
(34) Lewis, F. W.; Harwood, L. M.; Hudson, M. J.; Drew, M. G. B.; Hubscher-Bruder, V.; Videva, V.; Arnaud-Neu, F.; Stamberg, K.; Vyas, S. *Inorg. Chem.* **2013**, *52*, 4993.
(35) Hudson, M. J.; Boucher, C. E.; Braekers, D.; Desreux, J. F.; Drew, M. G.; Foreman, M. R. S. J.; Harwood, L. M.; Hill, C.; Madic, C.; Marken, F. *New J. Chem.* **2006**, *30*, 1171.
(36) Berthet, J.-C.; Maynadié, J.; Thuéry, P.; Ephritikhine, M. *Dalton Trans.* **2010**, *39*, 6801.
(37) Distler, P.; Spendlikova, I.; John, J.; Harwood, L.; Hudson, M.; Lewis, F. *Radiochim. Acta* **2012**, *100*, 747.
(38) Harwood, L. M.; Lewis, F. W.; Hudson, M. J.; John, J.; Distler, P. *Solvent Extr. Ion Exch.* **2011**, *29*, 551.
(39) Retegan, T.; Ekberg, C.; Dubois, I.; Fermvik, A.; Skarnemark, G.; Wass, T. J. *Solvent Extr. Ion Exch.* **2007**, *25*, 417.
(40) Kirker, I.; Kaltsoyannis, N. *Dalton Trans.* **2011**, *40*, 124.

(41) Nilsson, M.; Andersson, S.; Drouet, F.; Ekberg, C.; Foreman, M.; Hudson, M.; Liljenzin, J. O.; Magnusson, D.; Skarnemark, G. *Solvent Extr. Ion Exch.* **2006**, *24*, 299.
(42) Bader, R. F. W. *Atoms in Molecules: A Quantum Theory*; Clarendon Press: Oxford, U.K., 1990.
(43) Matta, C. F.; Boyd, R. J. *The quantum theory of atoms in molecules*; Wiley-VCH: Weinheim, Germany, 2007.
(44) Ingram, K. I.; Tassell, M. J.; Gaunt, A. J.; Kaltsoyannis, N. *Inorg. Chem.* **2008**, *47*, 7824.
(45) Tassell, M. J.; Kaltsoyannis, N. *Dalton Trans.* **2010**, *39*, 6719.
(46) Kerridge, A.; Coates, R.; Kaltsoyannis, N. *J. Chem. Phys.* **2009**, *113*, 2896.
(47) Kerridge, A.; Kaltsoyannis, N. *J. Phys. Chem. A* **2009**, *113*, 8737.
(48) Cukrowski, I.; Govender, K. K. *Inorg. Chem.* **2010**, *49*, 6931.
(49) Benay, G.; Schurhammer, R.; Wipff, G. *Phys. Chem. Chem. Phys.* **2011**, *13*, 2922.
(50) Berny, F.; Muzet, N.; Troxler, L.; Dedieu, A.; Wipff, G. *Inorg. Chem.* **1999**, *38*, 1244.
(51) Cao, X.; Heidelberg, D.; Ciupka, J.; Dolg, M. *Inorg. Chem.* **2010**, *49*, 10307.
(52) Chatterjee, T.; Sarma, M.; Das, S. K. *Cryst. Growth Des.* **2010**, *10*, 3149.
(53) Coupez, B.; Boehme, C.; Wipff, G. *Phys. Chem. Chem. Phys.* **2002**, *4*, 5716.
(54) Petit, L.; Adamo, C.; Maldivi, P. *Inorg. Chem.* **2006**, *45*, 8517.
(55) Petit, L.; Joubert, L.; Maldivi, P.; Adamo, C. *J. Am. Chem. Soc.* **2006**, *128*, 2190.
(56) Lan, J.-H.; Shi, W.-Q.; Yuan, L.-Y.; Zhao, Y.-L.; Li, J.; Chai, Z.-F. *Inorg. Chem.* **2011**, *50*, 9230.
(57) Narbutt, J.; Oziminski, W. P. *Dalton Trans.* **2012**, *41*, 14416.
(58) Becke, A. D.; Edgecombe, K. E. *J. Chem. Phys.* **1990**, *92*, 5397.
(59) Savin, A.; Nesper, R.; Wengert, S.; Fässler, T. F. *Angew. Chem., Int. Ed. Engl.* **1997**, *36*, 1808.
(60) Silvi, B.; Savin, A. *Nature* **1994**, *371*, 683.
(61) Foster, J. P.; Weinhold, F. *J. Am. Chem. Soc.* **1980**, *102*, 7211.
(62) Parr, R. G.; Yang, W. *Density Functional Theory of Atoms and Molecules*; Oxford University Press: New York, 1989.
(63) Becke, A. D. *J. Chem. Phys.* **1993**, *98*, 5648.
(64) Stephens, P. J.; Devlin, C. F.; Chabalowski, M. J.; Frisch, M. J. *J. Phys. Chem.* **1994**, *98*, 11623.
(65) Perdew, J. P.; Burke, K.; Ernzerhof, M. *Phys. Rev. Lett.* **1996**, *77*, 3865.
(66) Perdew, J. P.; Burke, K.; Ernzerhof, M. *Phys. Rev. Lett.* **1997**, *78*, 1396.
(67) Tao, J. M.; Perdew, J. P.; Staroverov, V. N.; Scuseria, G. E. *Phys. Rev. Lett.* **2003**, *91*, 146401.
(68) Frisch, M. J.; Trucks, G. W.; Schlegel, H. B.; Scuseria, G. E.; Robb, M. A.; Cheeseman, J. R.; Scalmani, G.; Barone, V.; Mennucci, B.; Petersson, G. A.; Nakatsuji, H.; Caricato, M.; Li, X.; Hratchian, H. P.; Izmaylov, A. F.; Bloino, J.; Zheng, G.; Sonnenberg, J. L.; Hada, M.; Ehara, M.; Toyota, K.; Fukuda, R.; Hasegawa, J.; Ishida, M.; Nakajima, T.; Honda, Y.; Kitao, O.; Nakai, H.; Vreven, T.; Montgomery, J. A.; Peralta, J. E.; Ogliaro, F.; Bearpark, M.; Heyd, J. J.; Brothers, E.; Kudin, K. N.; Staroverov, V. N.; Kobayashi, R.; Normand, J.; Raghavachari, K.; Rendell, A.; Burant, J. C.; Iyengar, S. S.; Tomasi, J.; Cossi, M.; Rega, N.; Millam, J. M.; Klene, M.; Knox, J. E.; Cross, J. B.; Bakken, V.; Adamo, C.; Jaramillo, J.; Gomperts, R.; Stratmann, R. E.; Yazyev, O.; Austin, A. J.; Cammi, R.; Pomelli, C.; Ochterski, J. W.; Martin, R. L.; Morokuma, K.; Zakrzewski, V. G.; Voth, G. A.; Salvador, P.; Dannenberg, J. J.; Dapprich, S.; Daniels, A. D.; Farkas, Ö.; Foresman, J. B.; Ortiz, J. V.; Cioslowski, J.; Fox, D. J. *Gaussian 09*; Gaussian, Inc.: Wallingford, CT, 2009.
(69) Réal, F.; Vallet, V.; Wahlgren, U.; Grenthe, I. *J. Am. Chem. Soc.* **2008**, *130*, 11742.
(70) Schlosser, F.; Krüger, S.; Rösch, N. *Inorg. Chem.* **2006**, *45*, 1480.
(71) Yang, T.; Bursten, B. E. *Inorg. Chem.* **2006**, *45*, 5291.
(72) Schreckenbach, G.; Hay, P. J.; Martin, R. L. *J. Comput. Chem.* **1999**, *20*, 70.
(73) Kaltsoyannis, N. *Chem. Soc. Rev.* **2003**, *32*, 9.
(74) Kaltsoyannis, N.; Hay, P. J.; Li, J.; Blaudeau, J.-P.; Bursten, B. E. In *The Chemistry of The Actinide and Transactinide Elements*; Morss, L. R., Edelstein, N. M., Fuger, J., Katz, J. J., Eds.; Springer: Dordrecht, The Netherlands, 2008; p 1893.
(75) Lan, J.-H.; Shi, W.-Q.; Yuan, L.-Y.; Li, J.; Zhao, Y.-L.; Chai, Z.-F. *Coord. Chem. Rev.* **2012**, *256*, 1406.
(76) Wang, D.; van Gunsteren, W. F.; Chai, Z. *Chem. Soc. Rev.* **2012**, *41*, 5836.
(77) Cao, X. Y.; Dolg, M.; Stoll, H. *J. Chem. Phys.* **2003**, *118*, 487.
(78) Küchle, W.; Dolg, M.; Stoll, H.; Preuss, H. *J. Chem. Phys.* **1994**, *100*, 7535.
(79) Hariharan, P. C.; Pople, J. A. *Theor. Chim. Acta* **1973**, *28*, 213.
(80) Lai, W.; Yao, J.; Shaik, S.; Chen, H. *J. Chem. Theory Comput.* **2012**, *8*, 2991.
(81) Ding, W.; Fang, W.; Chai, Z.; Wang, D. Submitted.
(82) Grimme, S.; Antony, J.; Ehrlich, S.; Krieg, H. *J. Chem. Phys.* **2010**, *132*, 154104.
(83) Barone, V.; Cossi, M.; Tomasi, J. *J. Comput. Chem.* **1998**, *19*, 404.
(84) Dapprich, S.; Frenking, G. *J. Phys. Chem.* **1995**, *99*, 9352.
(85) Gorelsky, S. I.; Ghosh, S.; Solomon, E. I. *J. Am. Chem. Soc.* **2006**, *128*, 278.
(86) Lu, T.; Chen, F. *J. Comput. Chem.* **2012**, *33*, 580.
(87) Allen, P. G.; Bucher, J. J.; Shuh, D. K.; Edelstein, N. M.; Reich, T. *Inorg. Chem.* **1997**, *36*, 4676.
(88) Combes, J. M.; Chisholm-Brause, C. J.; Brown, J. G. E.; Parks, G. A.; Conradson, S. D.; Eller, P. G.; Triay, I. R.; Hobart, D. E.; Meijer, A. *Environ. Sci. Technol.* **1992**, *26*, 376.
(89) Clark, D. L.; Keogh, D. W.; Palmer, P. D.; Scott, B. L.; Tait, C. D. *Angew. Chem., Int. Ed.* **1998**, *37*, 164.
(90) Tsushima, S.; Suzuki, A. *THEOCHEM* **2000**, *529*, 21.
(91) Vallet, V.; Wahlgren, U.; Schimmelpfennig, B.; Szabo, Z.; Grenthe, I. *J. Am. Chem. Soc.* **2001**, *123*, 11999.
(92) Gagliardi, L.; Roos, B. O. *Inorg. Chem.* **2002**, *41*, 1315.
(93) Vallet, V.; Privalov, T.; Wahlgren, U.; Grenthe, I. *J. Am. Chem. Soc.* **2004**, *126*, 7766.
(94) Schmider, H. L.; Becke, A. D. *THEOCHEM* **2000**, *527*, 51.